Thin Solid Films 539 (2013) 161–165

Contents lists available at SciVerse ScienceDirect

Thin Solid Films

journal homepage: www.elsevier.com/locate/tsf

Role of film thickness on the properties of ZnO thin films grown by sol-gel method

Vinod Kumar [a,b,f,*], Neetu Singh [c,d], R.M. Mehra [e], Avinashi Kapoor [c], L.P. Purohit [b], H.C. Swart [f]

[a] Materials Science Group, Inter University Accelerator Centre, Aruna Asaf Ali Marg, New Delhi-110 067, India
[b] Department of Physics, Gurukula Kangri University, Haridwar-249 404, India
[c] Department of Electronic Science, University of Delhi South Campus, New Delhi-110 021, India
[d] Department of Electronics, Keshav Mahavidyalaya, University of Delhi-110 034, India
[e] School of Engineering & Technology, Sharda University, Greater Noida-201 306, India
[f] Department of Physics, University of the Free State, Bloemfontein, ZA-9300, South Africa

ARTICLE INFO

Article history:
Received 24 October 2012
Received in revised form 14 May 2013
Accepted 17 May 2013
Available online 25 May 2013

Keywords:
Sol-gel
Zinc oxide
Thickness
Surface morphology
Solar cell and gas sensors

ABSTRACT

This paper reports the effect of thickness on the structural, morphological and optical properties of zinc oxide (ZnO) films. Thickness of ZnO films varied from 98 to 366 nm with an increase in the number of deposition cycles. Surface morphological studies showed that the increase in the film thickness causes an increase in the grain size. Roughness of the films has increased from 5.8 to 47 nm with an increase in the film thickness from 98 to 366 nm. The band gap is observed to vary from 3.33 to 3.24 eV with change in the film thickness from 98 to 366 nm. Thickness of the film affected the overall properties of the ZnO films significantly. The large surface roughness makes ZnO films to be potentially used as electrode in solar cells and gas sensing applications.

1. Introduction

ZnO is a group II–VI compound n-type semiconductor, with hexagonal wurtzite structure. ZnO has a direct band gap of 3.37 eV [1] and a large exciton binding energy of 60 meV at room temperature [2]. The microscopic surface topology and grain structure of transparent conducting films strongly affect the performance of solar cells. For such applications, the development of low resistive transparent conducting oxide (TCO) thin films along with textured surface is very important [3,4]. Presence of texture is an advantage for application in solar cells because scattering of light into the active layer of the cell is enhanced. This increases the optical path length [5] and consequently the generation of free carriers. ZnO is a promising material for optoelectronics [6,7], photovoltaics [8], sensors [9], data storage [10], biochemical/chemical sensors [11,12] and solid state lighting sources [13].

Nowadays, many physical and chemical techniques to grow ZnO thin film have been used such as spray pyrolysis [14], metal organic chemical vapor deposition [15], pulsed laser deposition [16], RF sputtering [17] and sol-gel technique [18]. Amongst the different available techniques, the sol-gel technique has the advantage of coating on large areas with easy control of the doping level, solution concentration and homogeneity, without using expensive and complicated equipments compared with the other methods. In the sol-gel process, the deposited films are in amorphous state, which are transformed into crystalline state during the annealing process. There are many factors affecting the crystallinity of the films such as the substrate, solution chemistry, heat treatment conditions and thickness etc. The optical and electrical properties are closely related to the crystallite size and orientation, which are affected by the film thickness.

Myoung et al. [19] have reported that the crystalline quality, electrical and optical properties of the ZnO films depend on the thickness. Reddy et al. [20] have reported the effect of film thickness on the structural, morphological and optical properties of ZnO films prepared by RF magnetron sputtering. For application in optoelectronic devices, normally the optimum film thickness is chosen for the best device performance. Therefore, it is very important to study the effect of film thickness on structural, morphological and optical properties of ZnO film. With this view in mind, in this paper, we present the effect of thickness variation on the structural, morphological and optical properties of ZnO films deposited on glass substrates by the sol-gel spin coating technique.

2. Experimental details

ZnO films on Corning (1737) substrates were deposited by the sol-gel method using the spin coating technique. Precursor solution of

* Corresponding author at: Department of Physics, University of the Free State, Bloemfontein, ZA9300, South Africa. Tel.: +27 848705159.
E-mail address: vinod.phy@gmail.com (V. Kumar).

0040-6090/$ – see front matter © 2013 Elsevier B.V. All rights reserved.
http://dx.doi.org/10.1016/j.tsf.2013.05.088

ZnO was prepared by dissolving zinc acetate dihydrate [$Zn(CH_3COO)_2.2H_2O$] (Merck) into ethanol (AR, Merck) and monoethanolamine (MEA, Merck) so as to prepare a concentration of 0.2 mol/l. MEA was then added in the solution. The molar ratio MEA/Zn was fixed to 1. The mixture was stirred ultrasonically at 25 °C for 2 h. A transparent and homogenous solution was obtained after 72 h (ageing time). A drop of the aged solution was put on an ultrasonically cleaned glass substrate, which was rotated at a speed of 2500 rpm for 30 s by a spin coater. After deposition, the film was dried in air at 230 °C for 10 min on a hot plate to evaporate the solvent and to remove organic residuals [18]. An approximate thickness of 19 nm was obtained for each spin. The above process of coating and drying was repeated several times to increase the film thickness. In the present work, the thickness of the films was varied in the range of 98-366 nm. The films were then annealed in air at 450 °C for 1 hour in a microprocessor controlled furnace with a heating rate of 5°/min.

The film thickness was measured with a surface profiler ambios XP-1. The crystalline nature of the ZnO films was confirmed by a PAN analytical X'pert PRO diffractometer using the CuK_α radiation having a wavelength of 1.5140 Å with Bragg–Brentano geometry. The scan speed was kept at 0.5° per minute with step size of 0.02°. The surface morphology of the films was investigated with scanning electron microscopy (SEM) (Zeiss EVO-40 EP). SEM operating voltage used in experiment is 25 keV. The topography of the ZnO films was analyzed by a Digital Nanoscope IIIa scanning probe microscopy. The band gap of ZnO films was measured by optical transmittance using a Shimadzu Solid Spec 3700 double beam spectrophotometer.

3. Results and discussion

3.1. Structural properties

Fig. 1 shows the thickness of the ZnO film as a function of the deposition cycles. The film thickness increased linearly with an increase in the number of cycles, representing a typical characteristic of the sol-gel spin coating technique. The X-ray diffraction (XRD) and SEM investigations give the information about the structure of the films. The preferred orientation of grains, grain size, stress, strain, etc can be obtained from the analysis of the Full Width at Half Maxima (FWHM), intensity and position of XRD peaks.

Fig. 2 shows the XRD pattern of ZnO films as a function of film thickness. The ZnO film with the lowest thickness (98 nm) has shown very low intensity. The intensity of ZnO films has increased continuously with an increase in film thickness from 98 to 366 nm.

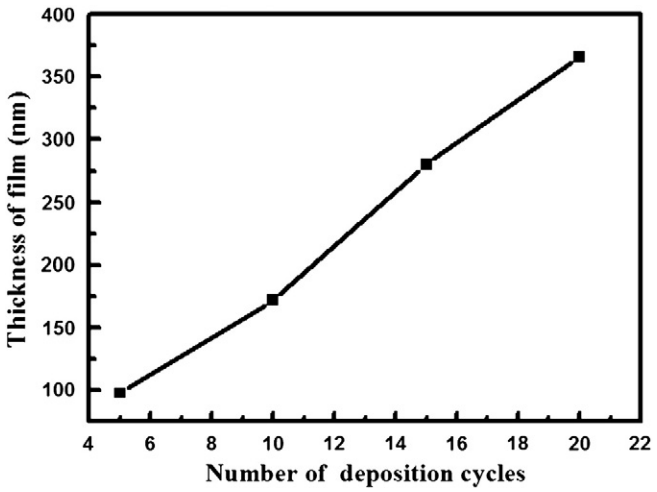

Fig. 1. Thicknesses of the film vs number of deposition cycles.

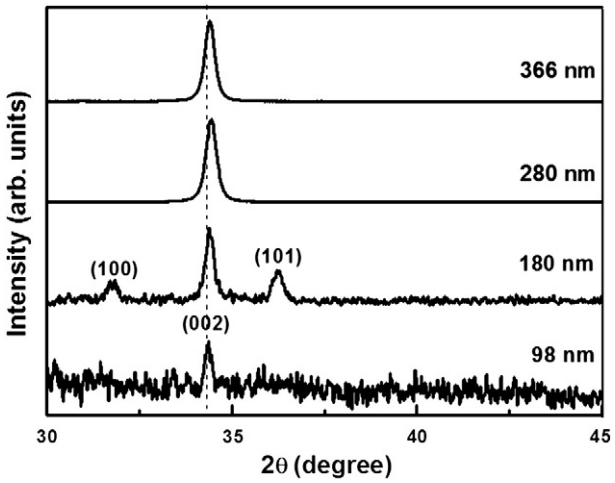

Fig. 2. X-ray pattern of the ZnO films for different ZnO thicknesses.

It is seen from the figure that as the film thickness increases from 98 to 366 nm, the intensity of the (002) peak increases and the width of the peak narrows. This suggests that as the film becomes thicker, the crystalline quality of the films is improved and the preferred orientation along the c-axis can be observed. The peak intensity and crystallite size are associated with the crystallinity of the films. Poor crystallinity in thinner ZnO film could be due to incomplete growth of crystallites [21]. According to the growth mechanism [22,23] the growing faces of crystallites correspond to the crystal shape. A growth competition starts among the neighboring crystals according to their orientation. Once the competition proceeds towards formation of same type of crystal faces, they form the free surface. This competitive growth mode represents an orientation selection [24]. This could be the reason of increased crystallinity with increase in thickness of the films. A similar behaviour was observed by Xu et al. in ZnO thin films synthesized by sol-gel [25].

The crystallite size as determined from the value of FWHM were calculated using Scherer's formula [26]

$$D = \frac{0.94\lambda}{B\cos\theta} \tag{1}$$

where λ, θ and B are the X-ray wavelength, Bragg's diffraction angle and FWHM of the ZnO (002) diffraction peak, respectively. The crystallite size of the ZnO films increased from 7 to 33 nm with an increase in film thickness from 98 to 366 nm. A similar behaviour was observed by Xu et al. in ZnO thin films synthesized by sol-gel [25]. The stress in the films was calculated by using the biaxial strain model [27]

$$\sigma = \frac{2C_{13}^2 - C_{33}(C_{11}+C_{12})}{C_{13}}\left(\frac{C_0 - C}{C}\right) \tag{2}$$

where C_{13}, C_{33}, C_{11}, C_{12} are elastic stiffness constants for ZnO. C_0 (0.52055 nm) is the strain-free lattice parameter measured from ZnO powder sample. C is the film lattice parameter and it varied from 0.52109 to 0.52024 nm with an increase in annealing temperature from 350 to 550 °C. The values of stiffness constants are C_{11} = 209.7 GPa, C_{12} = 121.1 GPa, C_{13} = 105.1 GPa, C_{33} = 210.9 GPa [28]. Stress in films can mainly be ascribed to two reasons; one is the intrinsic stress due to impurities and defects in crystal and other is extrinsic stress due to lattice mismatch, growth conditions and mismatch in the thermal expansion coefficient of the film and substrate. The value of stress in ZnO films are varied from −2.79 to 8.09 GPa with an increase

in film thickness from 98 to 366 nm. It can be noted that the nature of the stress in ZnO films is initially compressive, which becomes tensile with an increase in the film thickness.

3.2. Surface morphology

The surface morphology was studied from the SEM images. The SEM images of ZnO films with different thicknesses are shown in Fig. 3. The ZnO film of 98 nm thickness has not shown appreciable grains. Grain growth has started at 180 nm thickness. The surface morphology of the film at 280 nm thickness indicates the starting of the formation of nanoparticles of ZnO. The grain size of ZnO has increased from 85 to 100 nm with an increase in the thickness from 280 to 366 nm. SEM images of the films with higher thicknesses (280 and 366 nm) indicate that the films are composed of a dense packing of grains without any cracks, indicating good quality. Zhong et al. have reported [29] that with the increase in film thickness, the grain size increases and the grain shape changed from regular hexagonal sheet-like to wedge-shaped, even pyramidal.

The surface topography of the annealed films was observed by atomic force microscopy (AFM) in the tapping mode. Fig. 4 shows the AFM images of ZnO films scanned over an area of $2.0 \times 2.0\ \mu m^2$. It shows that hexagonally faceted columnar grains play a dominant role in the surface morphology. It can be observed that with an increase in thickness, the surface roughness of the films increased. For the film thickness of 98 nm the root mean square (RMS) roughness was 5.8 nm. With an increase of film thickness to 366 nm the RMS roughness has gradually increased to 47 nm. The increase of RMS roughness with the increase of film thickness was due to the larger grains formation as well as an increase in the porosity of the films [30]. The growth of a film undergoes several stages: nucleation, crystal growth and grain growth. Nucleation takes place on the surface of the substrate at the very first stage of condensation. In our study since the substrate was an amorphous structure, the nuclei formed were randomly oriented that's amorphous. The neighboring crystals compete with one other for growth to select a single orientation. The grains coalesce and grow in a direction to minimize the energy of the substrate-film interface and free surface energy. As a result grain boundaries become mobile and grow perpendicular to the film plane. In this layer by layer growth process, each of the spin coated layer act as a self template layer for the next coating. Wang et al. [31] have reported a single template formation and suggested that preferential orientation is a self assembly process induced by dipole-dipole interaction among the polar nanograins.

The high surface roughness of ZnO films is useful in solar cells as well as gas sensors. Lee et al. [32] have also reported that the bilayer AZO films have strong potential in TCO layers with light trapping function for thin film solar cells as they essentially combine high electrical conductivity and surface roughness (33 nm) of the top nanorod layer for the light trapping layer. The sensitivity and response time of ZnO based gas sensors strongly depends on the roughness of the thin film. Increase in film roughness increases the specific surface area suitable for gas adsorption and consequently, the sensor response [33].

3.3. Optical properties

Transmittance of ZnO films was measured in the wavelength range from 300 to 800 nm. The effect of film thickness on the optical properties such as transmittance and band gap of ZnO films was investigated. Fig. 5(a) shows the transmittance curves of ZnO films with different film thickness. All the samples showed good transparency higher than 84%. With increasing film thickness, the transmittance of the films decreased. Increase in transmittance can be explained with the help of the following relation

$$I = I_0 e^{-\alpha d} \tag{3}$$

where α is the absorption coefficient and d is the film thickness. Optical absorption coefficient (α) is calculated using [34]

$$\alpha = \frac{1}{d} \ln\left(\frac{1}{T}\right) \tag{4}$$

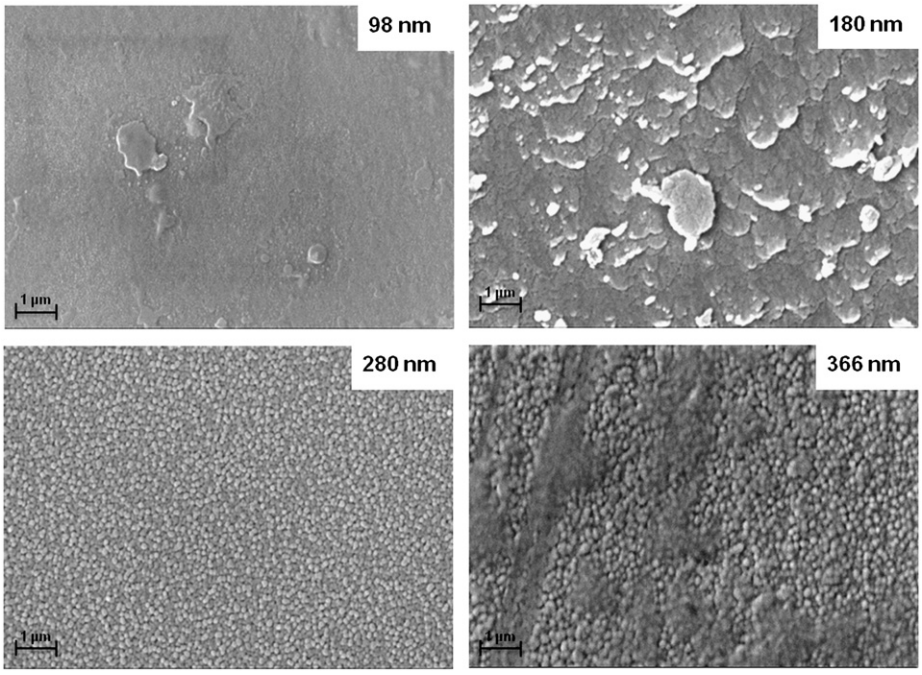

Fig. 3. SEM images of the different thickness ZnO thin films.

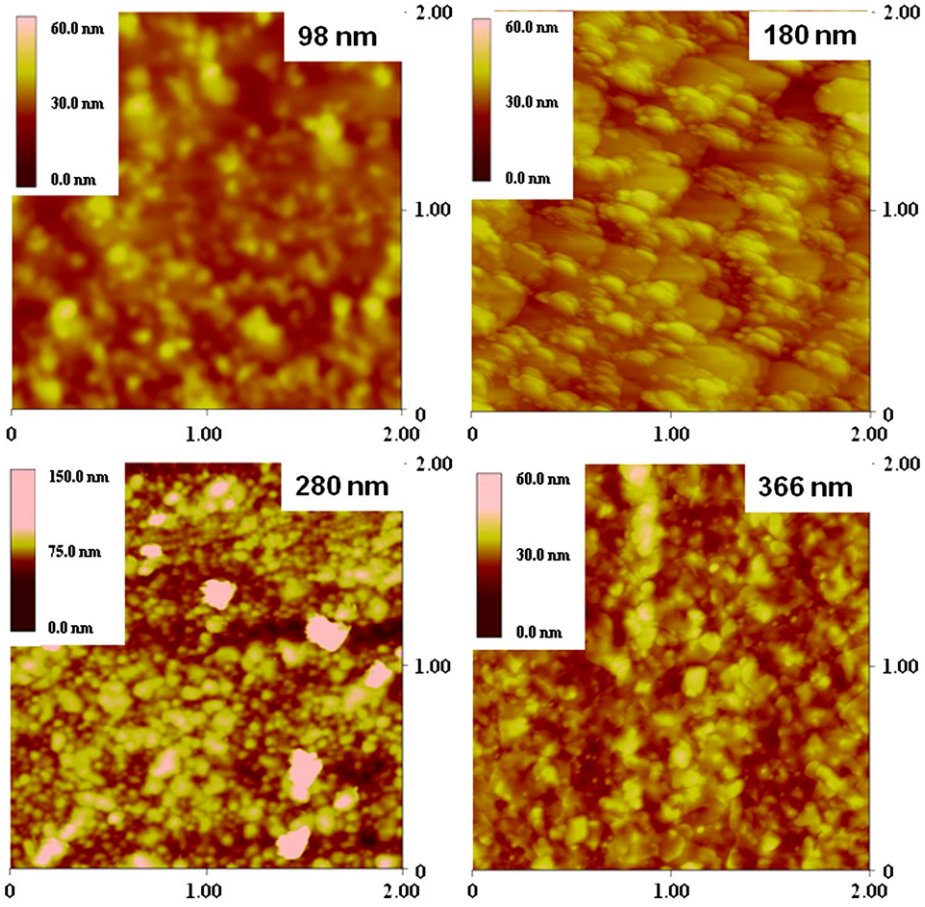

Fig. 4. AFM images of the different thickness ZnO thin films.

where T is the transmittance and d is the thickness of film. For the allowed direct transition, the variation of α with photon energy (hυ) obey Tauc's plot [34]

$$(\alpha h\nu)^2 = A\left(h\nu - E_g\right) \tag{5}$$

where E_g is the optical band gap, h is Planck's constant, α is the absorption coefficient and A is a constant having values between 1×10^5 and 1×10^6 cm^{-1} eV^{-1} [35]. Fig. 5(b) shows the Tauc's plot as a function of film thickness for the ZnO films. The band gap decreased from 3.33 to 3.24 eV with an increase in the film thickness. The decrease in the optical band gap with increase in film thickness is due to the variation in lattice defects and stress [36,37]. The compressed lattice is expected to provide a wide band gap because of the increased repulsion between the oxygen 2p and the zinc 4s bands.

4. Conclusion

High quality transparent ZnO films of different thickness were deposited by the sol-gel method using the spin coating technique. It was found that the crystallinity, surface morphology and optical properties of ZnO films depend strongly on the film thickness. Thus it can be concluded that the overall quality and the growth pattern of the films dependent on its thickness. The film having the highest surface

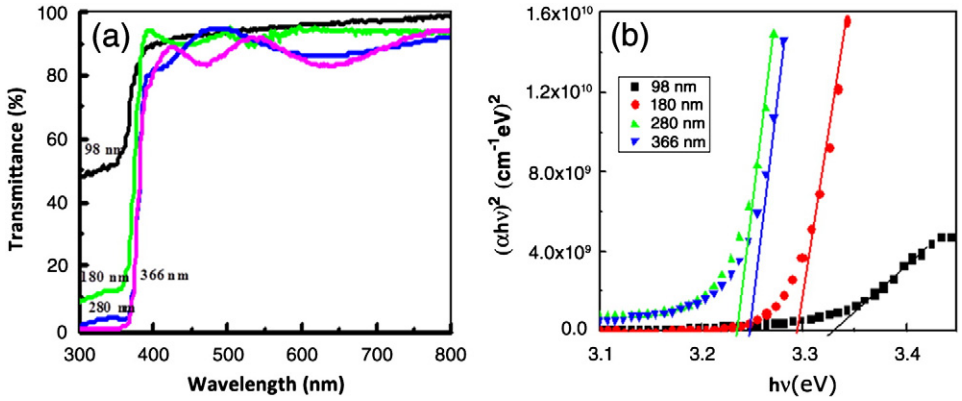

Fig. 5. Effect of film thickness on (a) transmittance and (b) band gap calculation using Tauc's plot.

roughness (47 nm) at 366 nm thickness is suitable for transparent conducting electrode in solar cells and gas sensor applications.

Acknowledgements

The authors wish to thank Dr. Jai Parkash Gupta, for AFM measurements.

References

[1] K. Nakahara, H. Takasu, P. Fons, A. Yamada, K. Iwata, K. Matsubara, R. Hunger, S. Niki, Appl. Phys. Lett. 79 (2001) 4139.
[2] J. Chen, T. Fujita, Jpn. J. Appl. Phys. 42 (2003) 602.
[3] H. Schade, Z.E. Smith, J. Appl. Phys. 57 (1985) 568.
[4] S. Major, K.L. Chopra, Sol. Energy Mater. 17 (1988) 319.
[5] C. Walker, R. Hollingsworth, J. Del Cueto, A. Madan, Mater. Res. Soc. Symp. Proc. 70 (1986) 563.
[6] X. Daun, Y. Huang, Y. Cui, J.F. Wang, C.M. Lieber, Nature 409 (2001) 66.
[7] H. Kind, H. Yan, M. Law, B. Messer, P. Yang, Adv. Mater. 14 (2002) 158.
[8] Neetu Singh, R.M. Mehra, Avinashi Kapoor, T. Soga, J. Renew. Sustain. Energy 4 (2012) 013110.
[9] C. Becker, F. Ruske, T. Sontheimer, B. Gorka, U. Bloeck, S. Gall, B. Rech, J. Appl. Phys. 106 (2009) 084506.
[10] F. Verbakel, Stefan C.J. Meskers, Rene A.J. Janssen, J. Appl. Phys. 102 (2007) 083701.
[11] Y. Cui, Q. Wei, H. Park, C.M. Lieber, Science 293 (2001) 1289.
[12] S.M. Al-Hilli, R.T. Al-Mofarji, P. Klason, M. Willander, N. Gutman, A. Saar, J. Appl. Phys. 103 (2008) 014302.
[13] M.D. Mc Cluskey, S.J. Jokela, J. Appl. Phys. 106 (2009) 071101.
[14] A. Goyal, S. Kachhwaha, Mater. Lett. 68 (2012) 354.
[15] J. Hu, R.G. Gordon, J. Appl. Phys. 71 (1992) 880.
[16] A. Suzuki, T. Matsushita, T. Aoki, Y. Yoneyama, M. Okuda, Jpn. J. Appl. Phys. 38 (1999) L71.
[17] Y. Kumar, J.E. Garcia, F. Singh, S.F. Olive-Méndez, V.V. Sivakumar, D. Kanjilal, V. Agarwal, Appl. Surf. Sci. 258 (2012) 2283.
[18] Vinod Kumar, R.G. Singh, L.P. Purohit, R.M. Mehra, J. Mater. Sci. Technol. 27 (2011) 481.
[19] J.M. Myoung, W.H. Yoon, D.H. Lee, I. Yun, S.H. Bae, S.Y. Lee, Jpn. J. Appl. Phys. 41 (2002) 28.
[20] R.S. Reddy, A. Sreedhar, A.S. Reddy, S. Uthanna, Adv. Mater. Lett. 3 (2012) 239.
[21] J.Y.W. Seto, J. Appl. Phys. 46 (1975) 5247.
[22] A. Van Der Drift, Philips Res. Rep. 22 (1967) 267.
[23] G. Knuyt, C. Quaeyhaegens, J.D. Haen, L.M. Stals, Phys. Status Solidi B 195 (1996) 179.
[24] P.B. Barna, M. Adamik, Thin Solid Films 317 (1998) 27.
[25] L. Xu, X. Li, Y. Chen, F. Xu, Appl. Surf. Sci. 257 (2011) 4031.
[26] B.C. Mohnaty, Y.H. Jo, D.H. Yeon, I.J. Choi, Y.S. Cho, Appl. Phys. Lett. 95 (2009) 062103.
[27] M.K. Puchet, P.Y. Timbrell, R.N. Lamb, J. Vac. Sci. Technol. A 14 (1996) 2220.
[28] T.B. Bateman, J. Appl. Phys. 33 (1962) 3309.
[29] A. Zhong, J. Tana, H. Huang, S. Chen, M. Wang, S. Xu, Appl. Surf. Sci. 257 (2011) 4051.
[30] N. Kakani, S.H. Jee, S.H. Kim, J.Y. Oh, Y.S. Yoon, Thin Solid Films 519 (2010) 494.
[31] J. Wang, Y. Qi, Z. Zhi, J. Guo, M. li, Y. Zhang, Smart Mater. Struct. 16 (2007) 2673.
[32] J.H. Lee, C.Y. Chou, Z. Bi, C.F. Tsa, H. Wang, Nanotechnology 20 (2009) 395704.
[33] S. Roy, S. Basu, Bull. Mater. Sci. 25 (2002) 513.
[34] A.E. Jimenez-Gonzalez, J.A.S. Urueta, R.J. Suarez-Parra, J. Cryst. Growth 192 (1998) 430.
[35] E.A. Davis, N.F. Mott, Philos. Mag. 22 (1970) 903.
[36] Y.C. Lin, B.L. Wang, W.T. Yen, C.T. Ha, C. Peng, Thin Solid Films 518 (2010) 4928.
[37] R. Ghosh, D. Basak, S. Fujihara, J. Appl. Phys. 96 (2004) 2689.